

sciendo

THE IMPACT OF MULTIFUNCTIONAL POLYSILOXANES ON ENHANCING THE PROPERTIES OF POLYETHYLENE TEREPHTHALATE GLYCOL (PET-G) FOR FDM/FFF 3D-PRINTING

Bogna SZTORCH*0, Julia GŁOWACKA*/**0, Miłosz FRYDRYCH*0, Daria PAKUŁA*0, Eliza ROMAŃCZUK-RUSZUK***®, Natalia KUBIAK*/**®, Robert E. PRZEKOP*®

*Centre for Advanced Technologies, Adam Mickiewicz University in Poznań, 10 Uniwersytetu Poznańskiego, 61-614 Poznań, Poland **Faculty of Chemistry, Adam Mickiewicz University in Poznań, 8 Uniwersytetu Poznańskiego, 61-614 Poznań, Poland ***Institute of Biomedical Engineering, Faculty of Mechanical Engineering, Bialystok University of Technology, Wiejska 45C Street, 15-351 Bialystok, Poland

bogna.sztorch@amu.edu.pl, julia.glowacka@amu.edu.pl, frydrych@amu.edu.pl, darpak@amu.edu.pl, e.romanczuk@pb.edu.pl, natalia.kubiak@amu.edu.pl, rprzekop@amu.edu.pl

received 27 December 2023, revised 03 April 2024, accepted 27 November 2024

Abstract: The use of incremental technologies in various biomedical fields requires the development of new materials that can meet the needs of new applications. This article delves into the impact of modifying PETG with multifunctional polysiloxanes (0.10 wt.% to 2.5 wt.%) on the properties of composite materials produced for 3D printing in bioengineering applications. The article covers the effects on strength (tensile, flexural), rheological (MFR), thermal (DSC), and surface (WCA) properties. The results obtained in this study indicate that polysiloxane additives have a positive effect on the material's elasticity and bending strength. Moreover, the results presented are a great example of interdisciplinary research combining chemical knowledge to develop specialized material applications.

Key words: PETG, polysiloxanes, 3D-printing, FDM/FFF, mechanical properties

1. INTRODUCTION

FDM/FFF 3D printing is gaining popularity and becoming more widely available as a tool for professional 3D printing facilities and home applications. It allows for fast and precise manufacturing and the creation of multipolymer-component systems with a wide range of materials. Obtaining physical prototypes through 3D FDM/FFF printing is guicker and more cost-effective than traditional manufacturing methods. In the event of failure of machine components, it allows the rapid manufacture of replacement parts, so that production does not have to be halted until replacement parts are made. 3D printing is also a tool that allows the development of creativity, which is why it is increasingly used by artists, clothing designers [1], and in education introduced as an element that shapes a new approach to shaping reality (giving nonobvious shapes) and exercising spatial imagination. This technology and other additive techniques will grow significantly in the coming years. However, additive techniques have limitations, including the current availability of printing materials on the market. which may not always meet the growing expectations of end users

Currently, FDM/FFF 3D printing is one of the most popular additive techniques that are used in various fields, such as automotive, submarines, aviation, and biomedical engineering. The increasing use of 3D printing in various fields is related to the possibility of creating elements with complex geometry and at the same time with good properties (low density, high mechanical properties) [3.4].

PETG (Polyethylene Terephthalate Glycol-Modified), where glycol-modified means that during the polymerization reaction, glycol was added but it is not included in the final product, is a popular 3D printing filament material stands out for its good mechanical properties, chemical stability, excellent aesthetic properties, and biocompatibility [5]. In addition, PET has high resistance to radiation and degradation in the presence of body fluids, which is why it is the most commonly used biomaterial [6]. Some of its uses include materials for orthodontic use, antibacterial films, scaffolds (tissue engineering), drugs, delivery, surgical models, etc [7-9]. However, like any material, it does have some weaknesses that users should be aware of: warping, stringing (tendency to produce thin strands or strings of filament between non-contiguous parts of the print), and hygroscopic. The flexibility of PET-G is good, but it may not be sufficient for more complex applications [10].

Polysiloxanes are a class of polymers that are also commonly known as silicones. They are made up of repeating units of siloxane (-R2Si-O-) where R represents various organic groups or hydrogen atoms. The general chemical formula for polysiloxanes is [(R2SiO)n], where "n" represents the number of repeating units in the polymer chain. Silicones are unique among polymers because they contain alternating silicon and oxygen atoms in their backbone, which gives them their distinctive properties. The organic groups attached to the silicon atoms determine the specific



Bogna Sztorch, Julia Glowacka, Milosz Frydrych, Daria Pakuła, Eliza Romańczuk-Ruszuk, Natalia Kubiak, Robert E. Przekop The Impact of Multifunctional Polysiloxanes on Enhancing the Properties of Polyethylene Terephthalate Glycol (Pet-G) for Fdm/Fff 3d-Printing

characteristics of the silicone polymer. Polysiloxanes/silicones have several notable properties, making them useful in various applications: high-temperature stability, flexibility and elasticity, water repellency, and transparency and optical clarity [11].

The literature contains publications on 3D printing of PETG filaments, but many of them focus on research on PETG-based composite materials. The analysis of the literature shows that there are no studies on the properties of PETG composites with polysiloxane modifiers. The most commonly used additives are carbon fibers or graphite and natural fiber [12,13,14]. Additives in the form of carbon fiber particles are added to improve the mechanical properties of the material [15,16]. In the work of Vijayasankar et al. [14] the properties of a 3D printed PETG composite with a natural filler were tested. Different percentages (2%, 5%, 10% by weight) of silk fibers were used. The research shows that the material with 2 % wt. silk increased the elastic modulus and compressive modulus compared to neat PETG. A printed prosthetic socket for the lower limb was presented as a possibility of using the material in biomedical engineering.

This study aimed to investigate how multifunctional polysiloxanes affect the properties of PETG for its suitability in FDM/FFF 3D printing technology. New polymer systems have been developed to address the limitations of 3D printing technology using PETG material. This system includes multifunctional polysiloxanes and PETG as the polymer matrix. The materials were modified with a series of polysiloxane-based derivates obtained by a hydrosilylation reaction.

2. MATERIALS AND METHODS

2.1. Materials

Polyethylene terephthalate glycol-modified (PET-G) copolyester type SELENIS SELEKT™ BD 110 (SELENIC NORTH AMERICA, LLC) The chemicals were purchased from the following sources: Polymethylhydrosiloxane, Trimethylsilyl Terminated (PWS) from Gelest, vinyl(trimetoxy)silane (VTMOS) (97%) from UNISIL; hexene (HEX), octene (OCT), allyl-glycidyl ether (AGE)) from Linegal Chemicals Warsaw, Poland, toluene from Avantor Performance Materials Poland S.A. Gliwice, Poland, and chloroform-d, Karstedt catalyst from Merck Group. In the process, toluene was dried and purified with MB SPS 800 Solvent Drying System and stored under an argon atmosphere in Rotaflo Schlenk flasks.

2.2. Synthesis of modifiers

Following the procedure described in the literature a 500 ml three-necked round bottom flask was filled with 30 g of PWS, 250 ml of toluene, and the appropriate amounts of olefins based on the number of moles of the Si-H moiety (see Tab. 1). A magnetic stirrer was then added to the flask. The reaction mixture was heated to 70°C and Karstedt's catalyst solution (8 x 10 -5 eq. Pt/mol SiH) was added. The reaction mixture was kept at reflux and samples were taken for FT-IR control until the Si-H signal disappeared completely (at 2141 and 889 cm-1). The solvent was removed under reduced pressure, resulting in an analytically pure sample.

Tab. 1. Polysiloxane derivatives

Core	Olefin 1	Olefin 2	Molar ratio
PWS	HEX	TMOS	2:1
PWS	OCT	TMOS	4:1
PWS	HEX	AGE	2:1
PWS	OCT	AGE	2:1

2.3. Filaments fabrication steps

For the masterbatch preparation, the polymer and the chosen additive were homogenized using a laboratory two-roll mill ZAMAK MERCATOR WG 150/280. A portion of 500 g PET-G was molten on the rolls, and then the additive was added in portions, until the final concentration of 5.0 wt.% (with respect to the whole system mass). The mixing was performed at the roll temperature of 225°C for 15 min, getting to full homogeneity of the composition. The resulting polymer system was then granulated using a SHINI SG-1417-CE grinding mill and dried at 55°C/24 h. After that, all of the prepared masterbatches were extruded using a twin-screw extruder machine to obtain final granulates. The granulates were diluted with neat PLA up to the final additive loading of 0.10, 0.25, 0.50, 1.0, 1.5, 2.5 wt.% upon screw extrusion with subsequent cold granulation on the extrusion setup HAAKE Rheomex OS in the processing temperature range 215-230°C, and then dried for 24 h at 55°C. The granulates obtained as above were used for the extrusion of filaments of 1.75 mm diameter by a single-screw extrusion setup FILABOT EX6. Extrusion temperatures were sequentially from the nozzle to the feed zone respectively: 190°C, 220°C, 220°C, and 80°C.

2.4. process by FDM/FFF technique

Using a 3D printer Prusa i3 MK3S+ two types of samples were printed: dumbbells and bars, according to PN-EN ISO 527. The parameters of printing are given in Table 2.

Tab. 2. 3D Printing process parameters

Parameter name	Parameter value
Layer height	0.18 mm
Top layer height	0.27 mm
Shells	2
Top and bottom layers number	3
Infill density	100%
Fill angle	45°
Infill pattern	Rectlinear grid
Printing speed	60 mm/s
Idle speed	80 mm/s
Extruder temp.	230°C
Table temp.	75°C

2.5. Methods and analyses

¹H, ¹³C, and ²⁹Si Nuclear Magnetic Resonance (NMR) spectra were recorded at 25°C on Bruker Ascend 400 and Ultra Shield 300 spectrometers using CDCl₃ as a solvent. Chemical shifts are



reported in ppm concerning the residual solvent (CHCl $_3$) peaks for ^1H and $^{13}\text{C}.$

Differential scanning calorimetry (DSC) was performed using a NETZSCH 204 F1 Phoenix (NETZSCH, Selb, Germany). Calorimeter samples of 5 ± 0.2 mg were cut and placed in an aluminum crucible with a punctured lid. The measurements were performed under nitrogen in the temperature range of -20–300°C and at a 20°C/min heating rate.

The effect of the modifier addition on the mass flow rate (MFR) was determined. The measurements were made using an Instron plastometer, model Ceast MF20 according to the applicable standard ISO 1133. The measurement temperature was 230 \pm 0.5°C, while the piston loading was 2.16 kg.

Static tensile and three-point bending tests were used to evaluate the mechanical behavior of PET-G composite 3D-printed samples. For flexural and tensile strength tests, the obtained materials were printed into type 1B and 1BA specimens by PN-EN ISO 527 and PN-EN ISO 178. Tests of the obtained specimens were performed on a universal testing machine INSTRON 5969 with a maximum load force of 50 kN. The traverse speed for tensile and flexural measurements was set at 2 mm/min. For all the series, 7 measurements were performed for each material.

Contact angle analyses were performed by the sessile drop technique at room temperature and atmospheric pressure, with a Krüss DSA100 goniometer. Three independent measurements were performed for each sample, each with a 5 μ l water drop, and the obtained results were averaged to reduce the impact of surface nonuniformity.

Light microscopy images of the printed samples were taken using a KEYENCE VHX-7000 digital microscope (Keyence International, Mechelen, Belgium, NV/SA) with a VH-Z100R wide-angle zoom lens at ×100-200 magnification.

3. RESULTS AND DISCUSSION

3.1. Characterization of synthesis products - NMR analysis

The synthesis procedure outlined in section 2.2 was followed to prepare the modifiers. In order to monitor the substrate conversion throughout the process, FT-IR analysis was employed. The reaction was carried out until the disappearance of the characteristic band (at 2141 and 889 cm-1) originating from the Si-H group of the precursor. In order to ascertain purity and determine the exact conversion, 1H NMR, 13C NMR, and 29Si NMR spectroscopy were also conducted. Based on 1H NMR analysis, the degree of conversion for all compounds was determined to be greater than 94%.

The product structures were confirmed by NMR spectroscopy, the following signals were assigned:

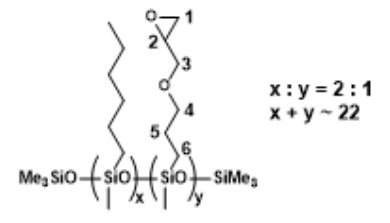


Fig. 1. PWS-2HEX-1AGE, Poly((hexylmethylsiloxane)-co-(3-propylglycidyl), trimethylsilyl terminated

¹H NMR (400 MHz, CDCl₃): δ (ppm) = 3.71-3.68 (m, position 3), 3.47-3.41 (m, position 3 and 4), 3.14 (m, position 2), 2.80-2.78 (m, position 1), 2.61 (m, position 1), 1.64-1.61 (m, position 5), 1.32-1.28 (m, hexyl -CH₂-), 0.90-0.88 (m, hexyl -CH₃), 0.54-0.53 (m, SiCH₂-), 0.13-0.06 (s, SiMe, SiMe₃)

¹³C NMR (101 MHz, CDCl₃): δ (ppm) = 74.23, 72.15, 71.53, 69.69, 50.95, 44.42 (AGE), 33.17, 31.77 (HEX), 23.35, 23.01 (AGE), 22.76, 17.70, 17.61, 17.46, 14.25 (HEX), 13.63, 13.51 (AGE), 1.98-1.51, -0.22-(-0.58) (SiMe, SiMe₃)

²⁹Si NMR ($\dot{7}9$,5 MHz, CDCl₃): δ (ppm) = -20.98-(-22.88) (SiMe, SiMe₃).

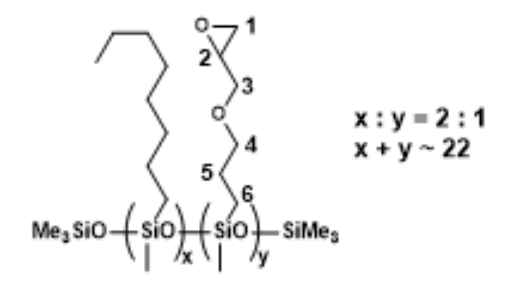


Fig. 2. PWS-2OKT-1AGE, Poly((methyloctylsiloxane)-co-(3-propylglycidyl), trimethylsilyl terminated

 1H NMR (400 MHz, CDCl₃): δ (ppm) = 3.72-3.68 (m, position 3), 3.50-3.40 (m, position 3 and 4), 3.17-3.13 (m, position 2), 2.82-2.79 (m, position 1), 2.63-2.60 (m, position 1), 1.69-1.62 (m, position 5), 1.34-1.30 (m, octyl -CH₂-), 0.93-0.89 (m, octyl -CH₃), 0.57-0.51 (m, SiCH₂-), 0.12-0.08 (SiMe₂)

¹³C NMR (101 MHz, CDCl₃): δ (ppm) = 74.30, 71.53, 50.94, 44.39 (AGE), 33.63, 33.55, 32.11, 29.57, 29.50 (OCT), 23.37, 23.21 (AGE), 22.83, 17.65, 17.54, 14.22 (OCT), 13.54, 13.44 (AGE), 1.98, 1.60, -0.19, -0.29, -0.47 (SiMe, SiMe₃);

²⁹Si NMR (79,5 MHz, CDCl₃): δ (ppm) = -21.28-(-23.45) (SiMe, SiMe₃).

$$\text{Me}_3 \text{SiO} \left(\frac{\text{SiO}}{x} \right)_x \left(\frac{\text{SiO}}{y} \right)_y \text{SiMe}_3 \qquad \begin{array}{c} \text{Si(OMe)}_3 & \text{produkt } \alpha \\ \text{x: } y = 2:1 \\ \text{x + } y \sim 26 \end{array} \right)$$

 α and β - 31:69

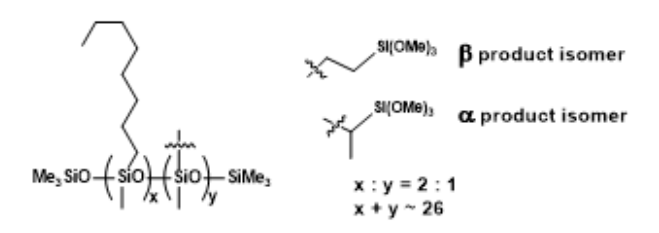
Fig. 3. PWS-2HEX-1TMOS, Poly((hexylmethylsiloxane)-co-(methyl(trimethoxyethyl)siloxane)), trimethylsilyl terminated (94% convertion)

¹H NMR (400 MHz, CDCl₃): δ (ppm) = 3.55 (s, OMe), 1.30-1.27 (m, hexyl -CH₂-), 1.09 (d, J=7.4Hz, α trimethylsiloxy), 0.87 (t, J=6.3Hz, hexyl -CH₃), 0.61-0.50 (m, SiCH₂-, SiCH(CH₃)Si), 0.14, 0.08, 0.06, 0.04 (s, SiMe₂, SiMe₃);

¹³C NMR (101 MHz, CDCl₃): δ (ppm) = 50.67, 50.61 (OMe), 33.28, 31.81, 23.19, 23.06, 22.80, 17.85, 14.24 (hexyl), 8.45 (Si-CH₂CH₂-Si), 7.60, 5.11 (SiCH(CH₃)Si), 1.98, 1.59, 0.67, -0.21, -1.14 (Si-CH₂CH₂-Si, SiMe₂, SiMe₃);

²⁹Si NMR (79,5 MHz, CDCl₃): δ (ppm) = -21.24-(-22.64) (SiMe, SiMe₃), -41.51-(-41.65) (Si(OMe)₃).





 α and β - 34:66

Fig. 4. PWS-2OCT-1TMOS, Poly((methyloctylsiloxane)-co-(methyl(trimethoxyethyl)siloxane)), trimethylsilyl terminated (94% conversion)

¹H NMR (400 MHz, CDCl₃): δ (ppm) = 3.56 (s, OMe), 1.30-1.27 (m, octyl -CH₂-), 1.09 (d, J=7.5Hz, α trimethylsiloxy), 0.88 (t, J=6.2Hz, octyl -CH₃), 0.61-0.50 (m, SiCH₂-, SiCH(CH₃)Si), 0.14, 0.08, 0.07, 0.04 (s, SiMe₂, SiMe₃);

¹³C NMR (101 MHz, CDCl₃): δ (ppm) = 50.65 (OMe), 33.31, 31.83, 23.18, 23.06, 22.80, 17.84, 14.25 (octyl), 8.42 (Si-CH₂CH₂-Si), 1.98, 1.58, 0.64, -0.22, -1.14 (Si-CH₂CH₂-Si, SiMe₂, SiMe₃); ²⁹Si NMR (79,5 MHz, CDCl₃): δ (ppm) = -21.22, -22.37-(-22.82) (SiMe, SiMe₃), -38.00, -41.54 (OSi(OMe)₃).

3.2. Mechanical behavior evaluation

To understand how additives affect the mechanical properties of composite materials, static mechanical tests on 3D FDM/FFF printed samples were conducted. The polysiloxane-based additives used strongly influenced the change in the mechanical characteristics of PET-G, because of their high plastification impact on polymeric materials similar to silsesquioxanes [17].

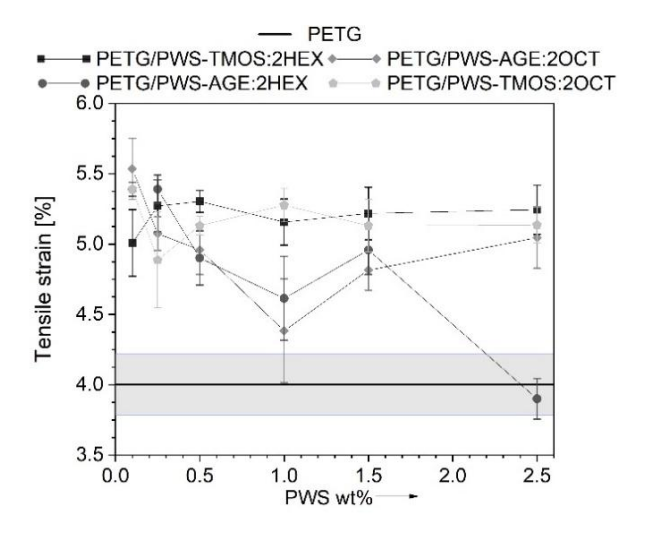


Fig. 5. Tensile strain (elongation at tensile strength) of PET-G and its composites as a function of polysiloxane-based modifier share

The mechanical results obtained from testing objects made with additive technology are not as straightforward as those produced through traditional methods of processing polymeric materials. This is due to the complexity of the additives used and the anisotropic nature of the objects' properties and defective structure resulting from their implementation, because of it all the results show a non-

linear trend. Results derived from static tensile tests are represented in Fig. 5-7. In Figure 5, it can be seen that materials with polysiloxane additions have higher tensile strain compared to neat PET-G. The exception is the material PETG/PWS-AGE:2HEX with 2.5% wt. modifier, that tensile strain is similar to neat PETG. The additives cause a strong plasticizing effect on the polymer matrix, as a result of which an increase in deformation of 35% compared to neat PET-G is observed. The presence of polysiloxanes in the polymer matrix indicates an increase in elastic properties which is attributed to their chemical structure. Polysiloxane's main chain is built with Si-O-Si, which is less restrictive and more flexible than the carbon-carbon C-C bounds found in carbon polymers. Side groups of polysiloxanes may also rotate around Si-O-Si bonds, contributing to their flexibility. In carbon polymers, such movements are typically more limited due to the less flexible carbon-carbon bonds [18]. The force-extension curve illustrates three distinct steps that correspond to the debonding of various sample layers and their deformation under axial tensile force (Fig. 6). The tensile strength (Fig. 7) of all tested materials with modifiers is worse compared to neat PET-G. The modifier particles penetrated the PET-G molecular chains, which reduced the intramolecular interactions between them and decreased their ability to resist tensile force. The addition of modifiers enhances the flexibility of the polymer matrix and negatively influences the tensile strength of the tested samples [19]. Only in the PETG/PWS-AGE:2HEX system, there is a slight improvement in tensile strength. This improvement may be due to the increased miscibility of the additive with the polymer matrix. The higher tensile strength could be attributed to the existence of epoxy groups in the glycidyl allyl. These groups potentially enhance the bonding between the different layers of the printed sample. Casarano et al. discussed the beneficial impact of allyl glycidyl ether on the properties of LMDPE/cellulose composites. They observed that the inclusion of AGE reduced the degree of crystallinity in the blends, acting as a plasticizer, and also enhanced interfacial interactions within the composites. Although there was a minor decrease in strength, the addition of AGE resulted in a noteworthy increase in elongation at break and improved adhesion between the two phases [20]. This phenomenon can be enhanced by the presence of hexane functional alkyl groups, which can also improve intermolecular adhesion.

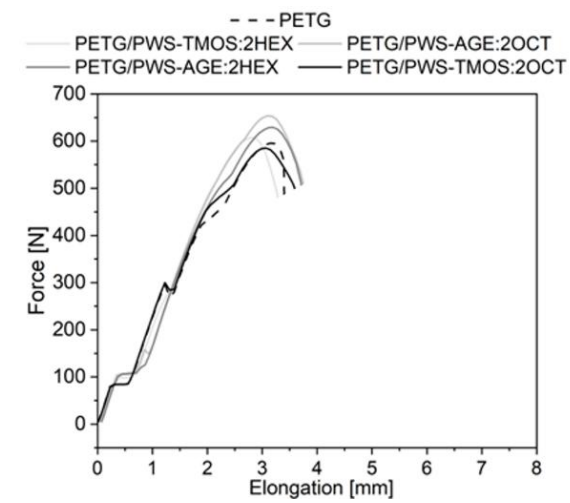


Fig. 6. Force vs elongation curves of PET-G and its composites



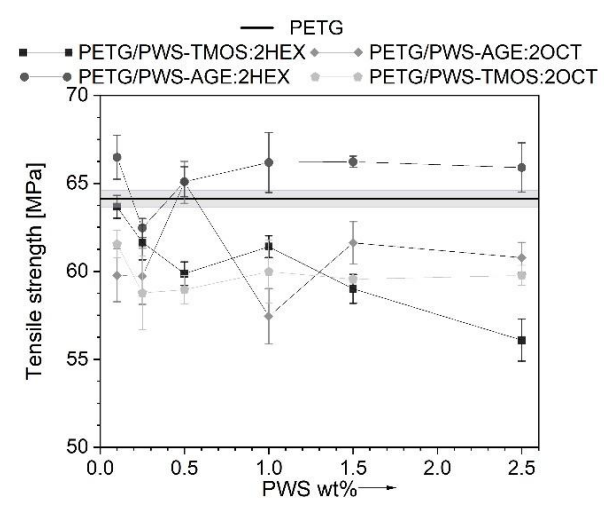


Fig. 7. Tensile strength of PET-G and its composites as a function of polysiloxane-based modifier share

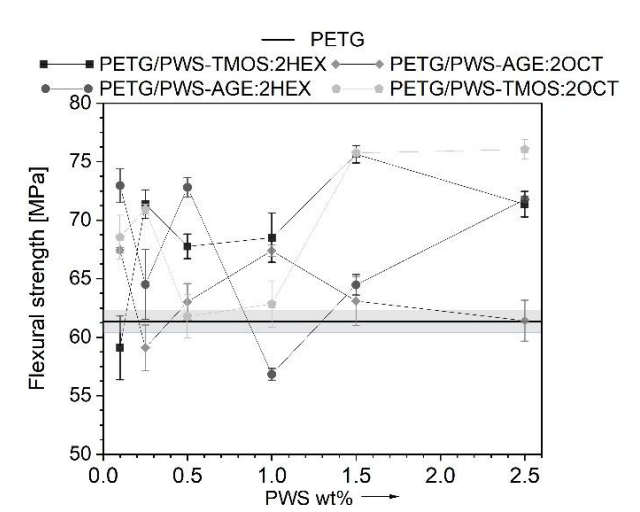


Fig. 8. Flexural strength of PET-G and its composites as a function of polysiloxane-based modifier share

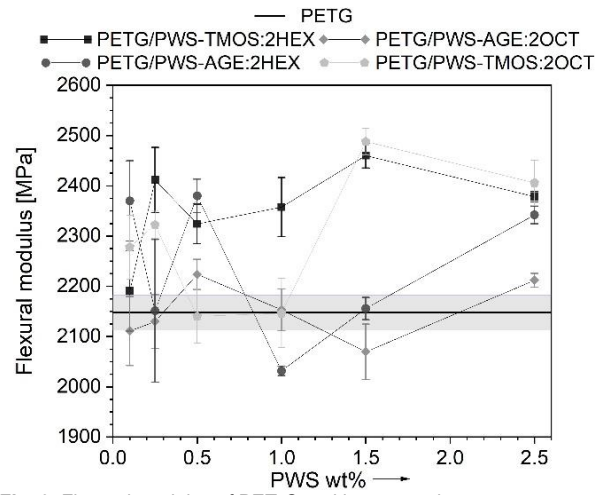


Fig. 9. Flexural modulus of PET-G and its composites as a function of polysiloxane-based modifier share

To assess the mechanical characteristics of the obtained composite materials and their ability to transfer bending loads, three-point bending mechanical tests were also carried out. The use of additives has notably enhanced the strength and bending

stiffness of the composites (Fig. 8-9). Glycidyl and trimethoxysilane groups can cause the formation of additional cross-links in the PET-G polymer structure, which can improve the material's flexural strength and stiffness [21]. Interactions between PET-G and polysiloxane additives' functional side groups can lead to a local increase in molecular entanglement and the formation of an interwoven network [22]. The change in flexural strength is greater than that in tensile strength, due to the different directions of load application and stress distribution resulting from the alignment of the print paths.

3.3. Rheological analysis

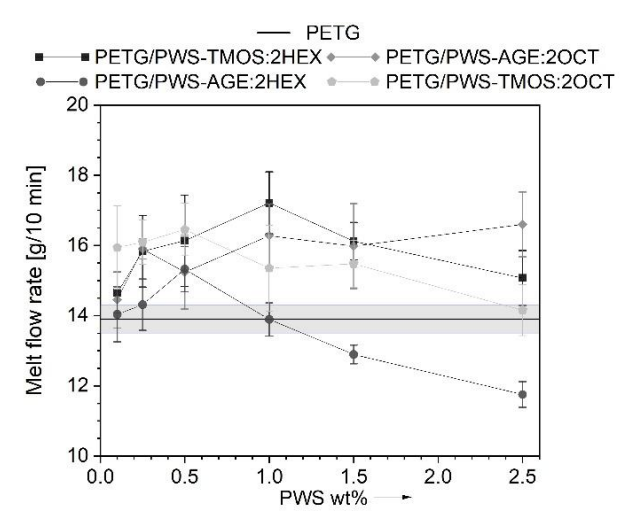


Fig. 10. Melt flow rate of PET-G and its composites as a function of polysiloxane-based modifier share

To evaluate the basic processing properties of PETG/PWS composites, mass flow rate (MFR) measurements were carried out. The results obtained are shown in Fig. 10. The additives used in small contents of up to 1% by weight have a positive effect on the change in the melt flow rate, which is due to the presence of alkylated substituents in the modifier molecule derived from hexene and octene allowing increased mobility of PET-G polymer chains. It promotes an increase in the MFR. Thus, these additives have the character of slip agents. Above 1% by weight of the additive, the lubricating character of the additives used arranges in a downward trend affecting the reduction of MFR, in the PETG/PWS-AGE:2HEX system, the MFR values are lower than the reference material (PET-G). It is related to the increasing proportion of glycidyl and trimethoxysilyl groups in the total volume of the composite, which, due to their similar polarity to the polymer matrix, can affect the stronger interaction of the modifier with the PET-G matrix.

3.4. Microscopic analysis

Microscopic images of sample fractures allow for a visual assessment of the adhesion level of the layers of the printed object. In the reference sample Fig. 11. 1A-1B, air gaps and clearly outlined layer boundaries can be seen. At the lowest concentration of 0.1%, no significant changes are visible compared to the reference sample (Fig. 11. series of images 1). This suggests that at this concentration, the material properties remain relatively consistent with the unmodified material. The modifiers PWS-



AGE:2OCT and PWS-TMOS:2HEX had a positive effect on the processability of materials (Section 3.3), increasing the MFR. Images Fig. 11. 2C and 2E exhibit smaller air gaps and improved interlayer adhesion, resulting in the disappearance of layer boundaries, which were visible in the reference sample.

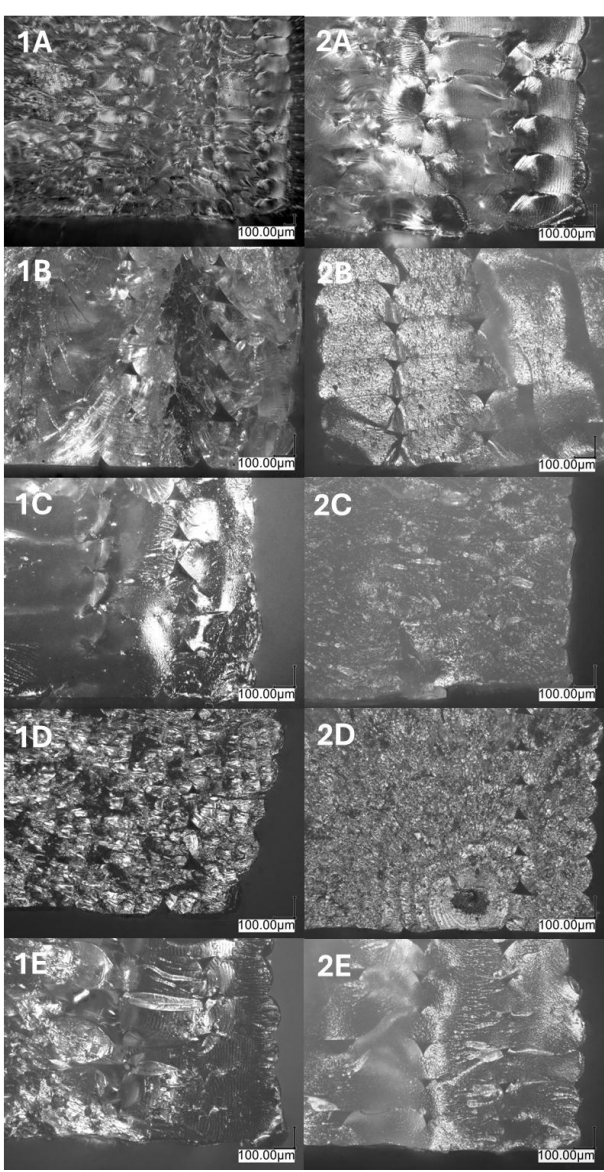


Fig. 11. Microscopic photos of sample fractures: 1A-2A Reference; 1B-0.1%, 2B-2.5% - PETG/PWS-AGE:2HEX; 1C-0.1%, 2C-2.5% - PETG/PWS-AGE:2OCT; 1D-0.1%, 2D-2.5% - PETG/PWS-TMOS:2OCT; 1E-0.1%, 2E-2.5% PETG/PWS-TMOS:2HEX

3.5. Water contact angle measurements (WCA)

In order to assess the impact of the polysiloxane-based additives with a concentration of 2.5% by weight in the composite systems on the surface properties of the 3D-printed samples, a test to measure the water contact angle on the surface was conducted. The measurement results are shown in Tab. 3. The value of the contact angle of the neat PET-G is 70.6°. It was observed that the addition of a modifier containing non-polar alkyl groups increases the degree of hydrophobicity of the tested samples. Visible effects are observed for the modifier using longer chain olefins, i.e. octene.

The contact angle increases by 14% and 25% for PETG/PWS-TMOS:4OCT composites with a longer alkyl chain and PETG/PWS-AGE:2OCT. For composites modified with polysiloxanes containing hexene substituents, the changes are insignificant.

Tab. 3. Contact angle measurement results for PET-G systems containing 2.5% polysiloxane-based additive

Name of the sample	Contact angle[°]
PET-G neat	70.6
PETG/PWS-TMOS:2HEX	73.4
PETG/PWS-TMOS:40CT	80.6
PETG/PWS-AGE:2HEX	75.8
PETG/PWS-AGE:20CT	88.2

3.6. Differential scanning calorimetry (DSC)

Figure 12 shows the results of differential scanning calorimetry (DSC) in inert gas flow. Neat PET-G and composite samples containing 2.5% modifier content were analyzed. The DSC curves (seen in Fig. 12) show only one endothermic peak in each sample, which corresponds to the glass transition temperature (Tg). PET-G belongs to amorphous polymers, therefore other transitions such as crystallization or melting are not observed. The unmodified sample has the highest glass transition temperature Tg = 86.3°C (Tab. 4). Organosilicon modifiers may have a plasticizing effect in polymer systems, which results in a lower glass transition temperature. The PETG/PWS-AGE:2OCT sample has the lowest Tg value. Glycidyl groups present in the modifier molecule affect the amorphization of the matrix material, which is also visible by changing the course of the DSC curve, for both PETG/PWS-AGE:2OCT and PETG/PWS-AGE:2HEX composite systems [23].

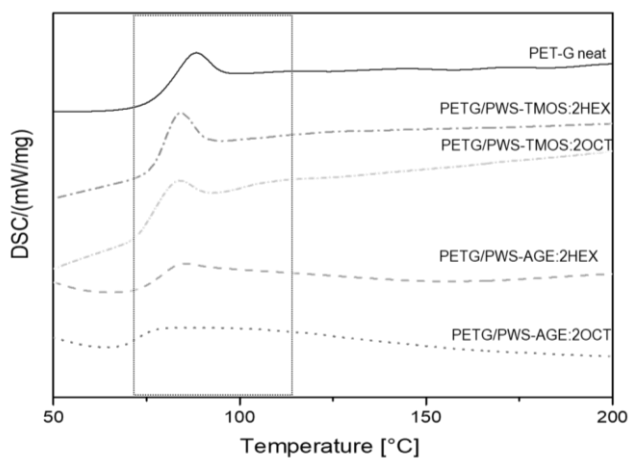


Fig. 12. DSC curves recorded for samples

Tab. 4. Results of DSC analysis

Name of the sample	Tg [°C]
PET-G neat	86.3
PETG/PWS-TMOS:2HEX	82.1
PETG/PWS-TMOS:20CT	80.4
PETG/PWS-AGE:2HEX	84.3
PETG/PWS-AGE:20CT	78.2



4. CONCLUSIONS

The field of biomedical engineering is constantly evolving, which calls for new solutions to meet the requirements for therapy, device construction, and materials. Additive technologies offer engineers design freedom due to the virtually unlimited spatial shaping possibilities, but materials and their properties can pose limitations. This study examines the impact of multifunctional polysiloxanes (ranging from 0.10 wt.% to 2.5 wt.%) on the properties of PETG for biomedical applications. Results show that the polysiloxane additives affect the plasticization of the polymer matrix, resulting in increased tensile flexibility of the composite materials. The addition of glycidic and trimethoxysilyl functional groups into the polysiloxane molecule also improves the bending strength properties. However, changes in strength properties were not clearly correlated with the concentration of the organosilicon modifier due to the anisotropic nature of 3D printed structures and the potential for internal defects. The analysis of the melt flow rate shows improved rheological properties of the composites, making them easier to process. Microscopic observations confirmed improvement in interlayer adhesion with increasing MFR. The hydrophobic nature of the polysiloxanes with octene groups increases the water contact angle of the print surface, reducing the negative impact of moisture on printed objects made from these composite materials.

REFERENCES

- Yap YL, Yeong WY. Additive manufacture of fashion and jewellery products: a mini review. Virtual Phys Prototyp. 2014;9(3):195–201.
- Shahrubudin N, Lee TC, Ramlan RJPM. An overview on 3D printing technology: Technological, materials, and applications. Procedia Manuf. 2019;35:1286–96.
- Calì M, Pascoletti G, Gaeta M, Milazzo G, Ambu R. New filaments with natural fillers for FDM 3D printing and their applications in biomedical field. Procedia Manuf. 2020;51:698–703.
- Pu'ad NM, Haq RA, Noh HM, Abdullah HZ, Idris MI, Lee TC. Review on the fabrication of fused deposition modelling (FDM) composite filament for biomedical applications. Mater Today Proc. 2020; 29:228–32.
- Hsueh MH, Lai CJ, Wang SH, Zeng YS, Hsieh CH, Pan CY, et al. Effect of printing parameters on the thermal and mechanical properties of 3D-printed PLA and PETG, using fused deposition modeling. Polymers (Basel). 2021;13(11).
- Gün Gök Z, İnal M, Bozkaya O, Yiğitoğlu M, Vargel İ. Production of 2hydroxyethyl methacrylate-g-poly(ethylene terephthalate) nanofibers by electrospinning and evaluation of the properties of the obtained nanofibers. J Appl Polym Sci. 2020;137(41).
- Szymczyk-Ziółkowska P, Łabowska MB, Detyna J, Michalak I, Gruber P. A review of fabrication polymer scaffolds for biomedical applications using additive manufacturing techniques. Biocybern Biomed Eng. 2020;40:624–38.
- Ping X, Wang M, Xuewu G. Surface modification of poly(ethylene terephthalate) (PET) film by gamma-ray induced grafting of poly(acrylic acid) and its application in antibacterial hybrid film. Radiat Phys Chem. 2011;80(4):567–72.
- Nicita F, D'Amico C, Filardi V, Spadaro D, Aquilio E, Mancini M, et al. Chemical-Physical Characterization of PET-G-Based Material for Orthodontic Use: Preliminary Evaluation of micro-Raman Analysis. Eur J Dent. 2023.
- Holcomb G, Caldona EB, Cheng X, et al. On the optimized 3D printing and post-processing of PETG materials. MRS Commun. 2022;12:381–7.
- 11. Zaman Q, Zia KM, Zuber M, et al. A comprehensive review on

- synthesis, characterization, and applications of polydimethylsiloxane and copolymers. Int J Plast Technol. 2019;23:261–82.
- García E, Núñez PJ, Caminero MA, Chacón JM, Kamarthi S. Effects of carbon fibre reinforcement on the geometric properties of PETGbased filament using FFF additive manufacturing. Compos B Eng. 2022;235.
- Kováčová M, Kozakovičová J, Procházka M, Janigová I, Vysopal M, Černičková I, et al. Novel Hybrid PETG Composites for 3D Printing. Appl Sci. 2020;10.
- Vijayasankar KN, Bonthu D, Doddamani M, Pati F. Additive Manufacturing of Short Silk Fiber Reinforced PETG Composites. Mater Today Commun. 2022;33:104772.
- Guessasma S, Belhabib S, Nouri H. Printability and Tensile Performance of 3D Printed Polyethylene Terephthalate Glycol Using Fused Deposition Modelling. Polymers (Basel). 2019;11(7).
- Alarifi IM. PETG/carbon fiber composites with different structures produced by 3D printing. Polym Test. 2023;120:107949.
- Brząkalski D, Sztorch B, Frydrych M, Pakuła D, Dydek K, Kozera R, et al. Limonene Derivative of Spherosilicate as a Polylactide Modifier for Applications in 3D Printing Technology. Molecules. 2020;25(24):5882.
- 18. Dvornic PR. Thermal properties of polysiloxanes. In: Silicon-containing polymers: the science and technology of their synthesis and applications. Dordrecht: Springer Netherlands; 2000. p. 185–212.
- Safandowska M, Rozanski A, Galeski A. Plasticization of Polylactide after Solidification: An Effectiveness and Utilization for Correct Interpretation of Thermal Properties. Polymers (Basel). 2020;12(3):561.
- Casarano R, Matos JDR, Fantini MCDA, Petri DFS. Composites of allyl glycidyl ether modified polyethylene and cellulose. Polymer (Guildf). 2005;46(10):3289–99.
- Przekop RE, Gabriel E, Pakuła D, Sztorch B. Liquid to Fused Deposition Modeling (L-FDM)—A Revolution in Application Chemicals to 3D Printing Technology—Mechanical and Functional Properties. Appl Sci. 2023;13(14):8462.
- 22. Pakuła D, Sztorch B, Romańczuk-Ruszuk E, Marciniec B, Przekop RE. High impact polylactide based on organosilicon nucleation agent. Chin J Polym Sci. 2024;1–11.
- 23. Obermeier B, Frey H. Poly(ethylene glycol-co-allyl glycidyl ether)s: A PEG-based modular synthetic platform for multiple bioconjugation. Bioconjug Chem. 2011;22(3):436–44.

Scientific research in the field of designing organosilicon modifiers of thermoplastic properties for the incremental FDM technique financed from the sources of the National Center for Research and Development under the LIDER X project (LIDER/01/0001 /L-10/18/NCBR/2019).

Bogna Sztorch: https://orcid.org/0000-0001-5166-8391

Julia Głowacka: https://orcid.org/0000-0003-1082-6714

Miłosz Frydrych: https://orcid.org/0000-0003-4196-5522

Daria Pakuła: https://orcid.org/0000-0001-6741-3019

Eliza Romańczuk-Ruszuk Dhttps://orcid.org/0000-0001-5228-4920

Natalia Kubiak: https://orcid.org/0009-0009-0536-4990

Robert E. Przekop: https://orcid.org/0000-0002-7355-5803



This work is licensed under the Creative Commons BY-NC-ND 4.0 license.